NUWC-NPT Technical Report 10,628
13 September 1996

Stability Measures for Spectral Analysis Using Discrete Sampling With the Kaiser-Bessel or Dolph-Chebyshev Window

Albert H. Nuttall
Surface Undersea Warfare Directorate

Jeffrey S. Hall
John V. Sanchis
Submarine Sonar Department

Naval Undersea Warfare Center Division
Newport, Rhode Island

PREFACE

The research in this report was sponsored by the Independent Research (IR) Program of the Naval Undersea Warfare Center (NUWC) Division, Newport, RI, under Project No. B10007, "Near-Optimum Detection of Random Signals With Unknown Locations, Structure, Extent, and Strengths," principal investigator Albert H. Nuttall (Code 311). The IR program is funded by the Office of Naval Research; the NUWC Division Newport program manager is Stuart C. Dickinson (Code 102). This effort was also sponsored by the Naval Sea Systems Command, program manager Thanh Nguyen (PMS 425243), under NUWC Division Newport Project No. E17653.

The technical reviewer for this report was Robert A. LaTourette (Code 2152).

Reviewed and Approved: 13 September 1996

Donald W. Counsellor
Head, Surface Undersea Warfare Directorate

REPORT DOCUMENTATION PAGE

Form Approved
OMB No. 0704-0188

1. AGENCY USE ONLY *(Leave blank)*	2. REPORT DATE	3. REPORT TYPE AND DATES COVERED
	13 September 1996	Final

4. TITLE AND SUBTITLE

Stability Measures for Spectral Analysis Using Discrete Sampling With the Kaiser-Bessel or Dolph-Chebyshev Window

5. FUNDING NUMBERS

6. AUTHOR(S)

Albert H. Nuttall
Jeffrey S. Hall
John V. Sanchis

7. PERFORMING ORGANIZATION NAME(S) AND ADDRESS(ES)

Naval Undersea Warfare Center Division
1176 Howell Street
Newport, RI 02841-1708

8. PERFORMING ORGANIZATION REPORT NUMBER

TR 10,628

9. SPONSORING/MONITORING AGENCY NAME(S) AND ADDRESS(ES)

Naval Sea Systems Command (PMS 425243)
2531 Jefferson Davis Highway
Arlington, VA 22242-5160

Office of Naval Research
800 North Quincy Street
Arlington, VA 22217-5000

10. SPONSORING/MONITORING AGENCY REPORT NUMBER

11. SUPPLEMENTARY NOTES

12a. DISTRIBUTION/AVAILABILITY STATEMENT

Approved for public release; distribution is unlimited.

12b. DISTRIBUTION CODE

13. ABSTRACT *(Maximum 200 words)*

Spectral estimation in sonar systems is usually performed by the classic weighted, overlap method. With this technique, the data to be analyzed are divided into overlapping sections. Each section is then weighted multiplicatively before it is fast Fourier transformed to the frequency domain. Next, all these magnitude-squared spectral estimates are averaged to produce the final estimate. As with all estimation techniques, the ratio of the mean to the standard deviation of the estimator should be as large as possible, which will ensure that a good spectral estimate "on the average" is obtained. In this report, an expression is derived for this important ratio called *stability*, which depends on only three quantities: the total number of data points T, the size of each section N, and the autocorrelation $\phi_w(m)$ of the discrete weighting function $w(n)$. The optimum overlap that maximizes stability for different values of T and N and for two commonly used windows (namely, Kaiser-Bessel and Dolph-Chebyshev) is computed. It is found that an overlap of 50 percent yields almost the same amount of stability as the optimal overlap for a wide variety of values of T, N, and $w(n)$.

14. SUBJECT TERMS

Discrete Sampling
Kaiser-Bessel Window
Dolph-Chebyshev Window
Power Spectral Estimation
Estimator Reliability
Sonar Systems

15. NUMBER OF PAGES
38

16. PRICE CODE

17. SECURITY CLASSIFICATION OF REPORT	18. SECURITY CLASSIFICATION OF THIS PAGE	19. SECURITY CLASSIFICATION OF ABSTRACT	20. LIMITATION OF ABSTRACT
Unclassified	Unclassified	Unclassified	SAR

TABLE OF CONTENTS

LIST OF ILLUSTRATIONS

LIST OF TABLES

LIST OF ACRONYMS

EDF	Expected Degrees of Freedom
FFT	Fast Fourier Transform
FO	Fractional Overlap

STABILITY MEASURES FOR SPECTRAL ANALYSIS USING DISCRETE SAMPLING WITH THE KAISER-BESSEL OR DOLPH-CHEBYSHEV WINDOW

1. INTRODUCTION

Power spectral estimation from a sample of a stationary random process has important detection and estimation applications in sonar. Consequently, we would like to obtain as accurate an estimate as possible (accurate meaning that the estimator has a low standard deviation relative to its mean). This measure of estimator reliability is known as *stability*; ideally then, we would like an estimate that is as stable as possible, given a finite sample of data.

The power spectrum estimator examined in this study is the standard overlapped fast Fourier transform (FFT) processor. With this method, a sliding weight function is applied multiplicatively to the data. The magnitude-squared FFTs of each weighted data segment are then summed to form the overall estimate.

The Kaiser-Bessel and Dolph-Chebyshev functions are used for the sliding weight. The Kaiser-Bessel window is characterized by a free parameter β that controls the peak sidelobe level and mainlobe width; the Dolph-Chebyshev window has the narrowest main lobe for a given peak sidelobe level. Both windows are thoroughly discussed in the classic Harris paper.[1]

Our primary objective is to determine the most stable estimate that can be obtained with the two different weightings; that is, what values of overlap (85, 90, 98 percent, etc.) will yield the highest stability measure? Rules of thumb are developed for establishing the optimal amount of overlap, based upon the two windows and their peak sidelobe levels. Moreover, since a 50-percent overlap is often used in practice, we derive the exact performance of this particular choice of processing (in terms of stability) relative to the optimum percentage overlap.

At the conclusion of this investigation, we find that although a 50-percent overlap is usually suboptimal, it often yields near-optimal stability.

2. DEFINITION AND INTERPRETATION OF EQUIVALENT DEGREES OF FREEDOM

Suppose that we have a set of J statistically independent, zero-mean Gaussian random variables $\{\boldsymbol{g}_j\}$ of common unknown power σ^2, which we wish to estimate. The best that we can do in this case is to compute the power estimate

$$\boldsymbol{\sigma}_e^2 \equiv \frac{1}{J}\sum_{j=1}^{J} \boldsymbol{g}_j^2 \,. \tag{1}$$

This quantity $\boldsymbol{\sigma}_e^2$ is an unbiased estimate of σ^2 since its mean, $\mathrm{Av}\{\boldsymbol{\sigma}_e^2\}$, is obviously σ^2, the desired quantity. At the same time, since variances of independent random variables add, the variance of the power estimate is

$$\mathrm{Var}\{\boldsymbol{\sigma}_e^2\} = \frac{1}{J}\,\mathrm{Var}\{\boldsymbol{g}_j^2\} \,. \tag{2}$$

And, since the fourth moment of Gaussian random variable $\boldsymbol{g}_j$ is $3\sigma^4$, the quantity in equation (2) is simply

$$\mathrm{Var}\{\boldsymbol{\sigma}_e^2\} = \frac{2\sigma^4}{J} \,, \tag{3}$$

which decays with J, the number of independent samples available. Naturally, we want J to be as large as possible, in order that the variance of the estimate $\boldsymbol{\sigma}_e^2$ be at a minimum.

Now consider the quality measure of estimate $\boldsymbol{\sigma}_e^2$, defined as the equivalent degrees of freedom,[2] namely,

$$\mathrm{EDF} \equiv \frac{2\,\mathrm{Av}^2\{\boldsymbol{\sigma}_e^2\}}{\mathrm{Var}\{\boldsymbol{\sigma}_e^2\}} = \frac{2\,(\sigma^2)^2}{2\sigma^4/J} = J \,, \tag{4}$$

where we have used equation (3). This ratio gives exactly the number of statistically independent samples available in the original data set $\{\boldsymbol{g}_j\}$. Therefore, it is natural and useful to consider extending the EDF definition in equation (4) to an arbitrary random variable $\boldsymbol{v}$ (formed *perhaps* as a sum of partially dependent random variables) as a measure of the effective number of independent contributors to $\boldsymbol{v}$. That is, we define, in general,

$$\mathrm{EDF} \equiv \frac{2\,\mathrm{Av}^2\{\boldsymbol{v}\}}{\mathrm{Var}\{\boldsymbol{v}\}} \tag{5}$$

for random variable $\boldsymbol{v}$. This statistic is attractive in that it only requires the calculation of the two lowest moments of $\boldsymbol{v}$. (If the mean of $\boldsymbol{v}$ is zero, the definition in equation (5) will have to be discarded; it is most meaningful when applied to estimates of power quantities, which are inherently positive.)

If random variable $\boldsymbol{v}$ depends on some parameter X, a search can be conducted on that parameter in an effort to maximize EDF, that is, minimize the standard deviation of $\boldsymbol{v}$ relative to its mean. In this way, the relative stability of estimate $\boldsymbol{v}$ can be optimized, subject, of course, to whatever constraints might have to be imposed on parameter X due to practical limitations.

3. STABILITY OF OVERLAP SPECTRAL ANALYSIS FOR DISCRETE SAMPLING

Stationary random process $\boldsymbol{x}(t)$ has correlation function $R_x(\tau) = \overline{\boldsymbol{x}(t)\boldsymbol{x}(t-\tau)}$ and (double-sided) power density spectrum $G_x(f)$. This process $\boldsymbol{x}(t)$ is sampled at increments of Δ seconds, where Δ should be chosen small enough to keep spectral aliasing under control; if not, we shall be estimating an excessively aliased spectrum instead of $G_x(f)$.* The data samples available are $\boldsymbol{x}(0), \boldsymbol{x}(\Delta), \ldots, \boldsymbol{x}((T-1)\Delta)$, for a total of T samples.

The total data record of T samples is broken up into segments of size N, which need not be a power of 2. Furthermore, these segments may overlap in time, thereby resulting in some data samples being processed in multiple segments. In addition, each data segment is weighted multiplicatively with a set of (delayed) coefficients, $w(0), w(1), \ldots, w(N-1)$, prior to being Fourier transformed, in order to control the sidelobe behavior of the windowed Fourier transform $W(f)$ associated with the set of weights. That is, window

$$W(f) \equiv \sum_{n=0}^{N-1} w(n) \exp(-i2\pi f \Delta n) \quad \text{for all } f\,, \tag{6}$$

which has period $1/\Delta$ in frequency f.

The segmenting and weighting procedure applied to the available data is illustrated in figures 1 and 2. The total number of pieces averaged in obtaining the power density spectrum estimate is P, which can vary over a wide range (under our control). The pth piece of weighted data is subjected to the (integer) shift S_p, where $1 \leq p \leq P$. In particular, we will choose $S_1 = 0$, in order to cover the first data sample $\boldsymbol{x}(0)$. Also, we will choose $S_P = T - N$, so that the last data segment covers the last available data sample $\boldsymbol{x}((T-1)\Delta)$. Figure 1 shows the case where the data segments do not overlap; figure 2 shows the case where the data segments do overlap because a large number of segments (large P) have been used. Note also from figure 2 that all the data points may not be used, depending upon the relationship between N, T, and P.

*This requirement for the sampling rate Δ is equivalent to the Nyquist sampling requirement in the frequency domain.

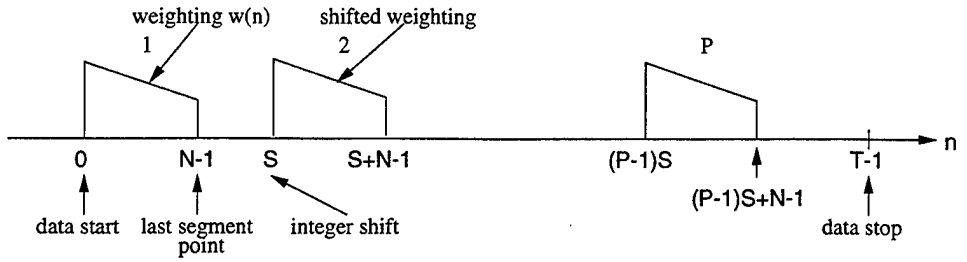

Figure 1. *Weighted and Overlapped Data Segments (Nonoverlapping Case)*

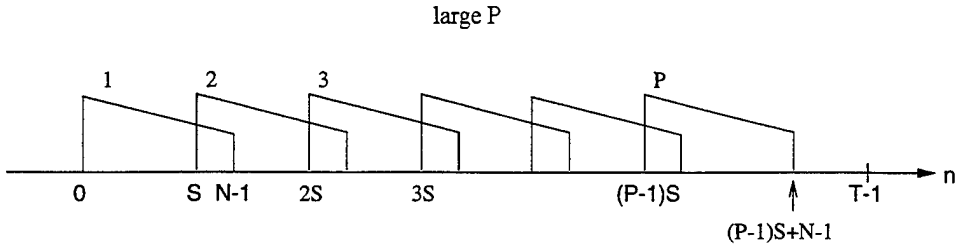

Figure 2. *Weighted and Overlapped Data Segments (Overlapping Case)*

In order to maximize the stability (minimize the variance) of the spectral estimate, we want to separate the P individual data segments as much as possible; that is, we want to minimize the amount of overlap of the individual segments. We accomplish this by first defining the (noninteger) quantity

$$S_c = \frac{T-N}{P-1}\,; \tag{7}$$

multiples of this shift would result in all the P segments being equally spaced. However, since S_c and its multiples are not integers, we will adopt the closest integer spacing for the shifts $\{S_p\}$ according to the rule

$$S_p \equiv \lceil (p-1)S_c \rceil \quad \text{for } 1 \le p \le P\,, \tag{8}$$

where $\lceil v \rceil$ denotes the closest rounded integer to v. As special cases, we have $S_1 = 0$ and $S_P = T - N$.

For arbitrary analysis frequency f_k, the pth voltage density estimate (using weighted sampled overlapped data) is defined as the complex quantity

$$\boldsymbol{y}_p(f_k) \equiv \sum_n \boldsymbol{x}(n\Delta)\, w\,(n - S_p)\, \exp\,(-i2\pi f_k n\Delta) \quad \text{for } 1 \le p \le P\,; \tag{9}$$

the limited nonzero range of the weights, $w(0)$ to $w(N-1)$, will automatically terminate the infinite summation in equation (9) at limits S_p to $S_p + N - 1$, as shown in figure 1. (If we choose to take $f_k = k/(K\Delta)$, where K is a power of 2, then equation (9) can be accomplished as a K-point FFT. Also, FFT size K can be chosen larger than segment length N[†] to realize interpolated values of the spectral estimate at frequency increment $(K\Delta)^{-1}$ of specified fineness.)

The power density spectrum estimate at frequency f_k is now derived from equation (9) as the finite average

$$\boldsymbol{Y}(f_k) \equiv \frac{1}{P} \sum_{p=1}^{P} \left| \boldsymbol{y}_p(f_k) \right|^2 . \tag{10}$$

We are interested in the mean and standard deviation of random variable $\boldsymbol{Y}(f_k)$ and, in particular, in the stability measure known as the EDF, namely,

$$\mathrm{EDF} \equiv \frac{2\,\mathrm{Av}^2\{\boldsymbol{Y}(f_k)\}}{\mathrm{Var}\{\boldsymbol{Y}(f_k)\}} . \tag{11}$$

For given values of T and N, the value of EDF will depend on P, the number of pieces in figure 1 and in the estimate of equation (10). We wish to make EDF as large as possible to minimize the variance and yet maintain P within reasonable bounds. Too small a value of P results in incomplete use of the available data; see figure 1 for an illustration of the nonoverlapping case. On the other hand, too large a value of P results in excessive overlap and an attendant amount of unnecessary calculations with little additional reduction in variance. The average fractional overlap (FO) of the segments is available from equation (7) as

$$\mathrm{FO} \equiv \max\left(\frac{N - S_c}{N}, 0\right) = \max\left(1 - \frac{S_c}{N}, 0\right) . \tag{12}$$

For example, assume that $T = 1024$ total data points and that the data segments consist of $N = 128$ data points. If $P = 8$ segments were desired, then $S_c = (1024 - 128)/(8 - 1) = 896/7 = 128$ from equation (7) and $\mathrm{FO} = 0$ from equation (12). This result clearly shows that $P = 8$ segments of 128 points each

[†]The additional $K - N$ data points all have zero value; this procedure is known as zero padding.

can be obtained from 1024 total points without any overlap. If P is now changed from 8 to 16, then S_c becomes $896/15 \approx 59.67$, and FO becomes 0.53, since with 16 pieces of 128 points each, there must be overlap if there are only 1024 total data points available.[‡]

The EDF is evaluated in appendix A, with the result that

$$EDF = \frac{2P^2}{\sum_{p,q=1}^{P} \left| \frac{\phi_w(S_q - S_p)}{\phi_w(0)} \right|^2}, \tag{13}$$

where $\phi_w(m)$, the autocorrelation of the weight sequence, is

$$\phi_w(m) \equiv \sum_n w(n)\, w(n-m) \quad \text{for all } m\,. \tag{14}$$

This sequence, $\{\phi_w(m)\}$, is zero for $|m| \geq N$, since $\{w(n)\}$ is of length N. Shifts $\{S_p\}$ are available from equations (7) and (8) for each choice of P.

The detailed spectrum $G_x(f)$ of random process $\boldsymbol{x}(t)$ does not appear in the end result for the EDF in equation (13), nor does the particular analysis frequency f_k. The reason for this behavior is our presumption that the magnitude-squared window $|W(f)|^2$ has a mainlobe width which is narrower than the detail in the spectrum $G_x(f)$ in the neighborhood of f_k and that the sidelobes of the window $W(f)$ in equation (6) are rather small.[§] Both these properties can be achieved by the selection of a large enough segment duration, $N\Delta$, and by the use of windows, $W(f)$, with good sidelobes, such as can be achieved from the Kaiser-Bessel or Dolph-Chebyshev weightings $\{w(n)\}$.

We can now concentrate on maximizing the quality ratio EDF in equation (13) by the choice of the number of pieces P, knowing that this will minimize the standard deviation of the spectral estimate $\boldsymbol{Y}(f_k)$ relative to its mean value.

[‡]It must be noted that the amount of FO available in actual sonar systems is often restricted to values such as 0.5, 0.75, and 0.875. Thus, an FO of 0.53, as discussed in the last example, may not be possible in practice.

[§]This is a reasonable assumption for practical FFT spectral estimation processes.

4. RULES OF THUMB

The following tables show the optimum overlap for maximizing stability measure EDF and indicate what fraction of this maximal amount is achieved for 50-percent overlap. From these tables, it can be seen that the following rules of thumb apply.

First, tables 1 and 2 show in the fifth column that the optimum overlap required to achieve maximum EDF is directly affected by the desired sidelobe level, data length T, and segment size N. As the sidelobe level decreases, the amount of overlap required for maximum EDF increases. These two tables also indicate (see the eighth column) that for both the Dolph-Chebyshev and Kaiser-Bessel windows, 50-percent overlap provides near optimum EDF, especially for shallower sidelobe levels (selectable by the parameter β for Kaiser-Bessel).

Figures 3 through 6 also illustrate a rule of thumb, which relates to how the EDF changes as a function of overlap for the Kaiser-Bessel weightings and four different peak sidelobe levels. For example, figure 4 shows EDF as a function of the number of pieces (sections) for a Kaiser-Bessel window designed for a -40 dB peak sidelobe level with $T = 1024$ and $N = 128$. For this example, the maximum EDF value of 29.42 is attained at FO = 0.632 (20 sections). The EDF value at 50-percent overlap is 27.82, resulting in a loss of only 5.4 percent relative to the maximum EDF value obtained at the optimal overlap. It is obvious that once the knee of the curve has been attained, further increases in the fractional overlap have little effect on improving EDF (i.e., obtaining better spectral estimates).

Another general rule can be summarized as follows: for a given N and T, EDF increases with deeper sidelobe levels. Thus, we expect a larger value of EDF for a peak sidelobe level of -60 dB than for a peak sidelobe level of -30 dB. The validity of this last statement can be verified by examination of tables 1 and 2.

It is helpful to have a simple rule of thumb to obtain the maximum value of EDF that can be realized for the two windows considered here. Accordingly, we have extracted the following approximation from the examples in tables 1 and 2. It is based upon reference 3 and is a function of the ratio T/N, namely, the ratio of the total number of data points to the length of the segments employed. It was obtained by fitting the empirical examples in tables 1 and 2 by a straight line in the

Table 1. *Optimum Overlap, Maximum EDF, and EDF Attainable at 50-Percent Overlap for Kaiser-Bessel Weighting*

SLL (dB)	T	N	T/N	Optimum Overlap	Max EDF	Max EDF T/N	Fraction at 50% Overlap
-30	512	128	4	0.57	12.2	3.05	0.99
-30	1024	128	8	0.59	26.1	3.26	0.99
-30	2048	128	16	0.61	53.8	3.36	0.98
-30	2048	256	8	0.59	26.0	3.25	0.99
-30	4096	128	32	0.62	109.2	3.41	0.98
-30	8192	1024	8	0.59	25.9	3.24	0.99
-40	512	128	4	0.63	13.7	3.42	0.96
-40	1024	128	8	0.63	29.4	3.68	0.95
-40	2048	128	16	0.66	61.0	3.81	0.94
-40	2048	256	8	0.63	29.3	3.67	0.95
-40	4096	128	32	0.67	124.1	3.88	0.94
-40	8192	1024	8	0.63	29.3	3.66	0.95
-50	512	128	4	0.67	14.9	3.73	0.91
-50	1024	128	8	0.68	32.3	4.04	0.89
-50	2048	128	16	0.69	67.2	4.20	0.89
-50	2048	256	8	0.68	32.2	4.03	0.90
-50	4096	128	32	0.71	137.0	4.28	0.88
-50	8192	1024	8	0.68	32.1	4.02	0.90
-60	512	128	4	0.70	16.0	4.01	0.86
-60	1024	128	8	0.71	34.9	4.37	0.84
-60	2048	128	16	0.73	72.8	4.55	0.84
-60	2048	256	8	0.71	34.8	4.35	0.85
-60	4096	128	32	0.74	148.6	4.64	0.83
-60	8192	1024	8	0.71	34.7	4.34	0.85

Table 2. *Optimum Overlap, Maximum EDF, and EDF Attainable at 50-Percent Overlap for Dolph-Chebyshev Weighting*

SLL (dB)	T	N	T/N	Optimum Overlap	Max EDF	Max EDF / T/N	Fraction at 50% Overlap
-30	512	128	4	0.57	12.2	3.1	0.99
-40	1024	128	8	0.59	26.4	3.3	0.98
-40	8192	1024	8	0.88	27.0	3.4	0.96
-40	2048	128	16	0.63	54.4	3.4	0.98
-40	16384	1024	16	0.84	54.5	3.4	0.95
-40	4096	128	32	0.65	110.6	3.5	0.98
-40	32768	1024	32	0.74	114.0	3.6	0.95
-50	1024	128	8	0.63	29.1	3.6	0.95
-50	2048	128	16	0.66	60.3	3.8	0.95
-50	4096	128	32	0.67	122.7	3.8	0.94
-50	2048	256	8	0.63	29.0	3.6	0.95
-50	2048	512	4	0.63	13.5	3.4	0.96
-50	8192	1024	8	0.63	29.0	3.6	0.95
-50	2048	128	16	0.66	60.3	3.8	0.95
-50	16384	1024	16	0.66	60.0	3.8	0.95
-50	4096	128	32	0.67	122.7	3.8	0.94
-50	32768	1024	32	0.68	122.1	3.8	0.94
-60	1024	128	8	0.67	31.6	4.0	0.91
-60	8192	1024	8	0.67	31.4	3.9	0.91
-60	2048	128	16	0.69	65.7	4.1	0.90
-60	16384	1024	16	0.69	65.3	4.1	0.90
-60	4096	128	32	0.70	133.9	4.2	0.90
-60	32768	1024	32	0.70	133.1	4.2	0.90
-70	1024	128	8	0.70	34.0	4.3	0.86
-70	8192	1024	8	0.70	33.8	4.2	0.87
-70	2048	128	16	0.71	70.7	4.4	0.86
-70	16384	1024	16	0.71	70.3	4.4	0.86
-70	4096	128	32	0.73	144.2	4.5	0.85
-70	32768	1024	32	0.72	143.4	4.5	0.86

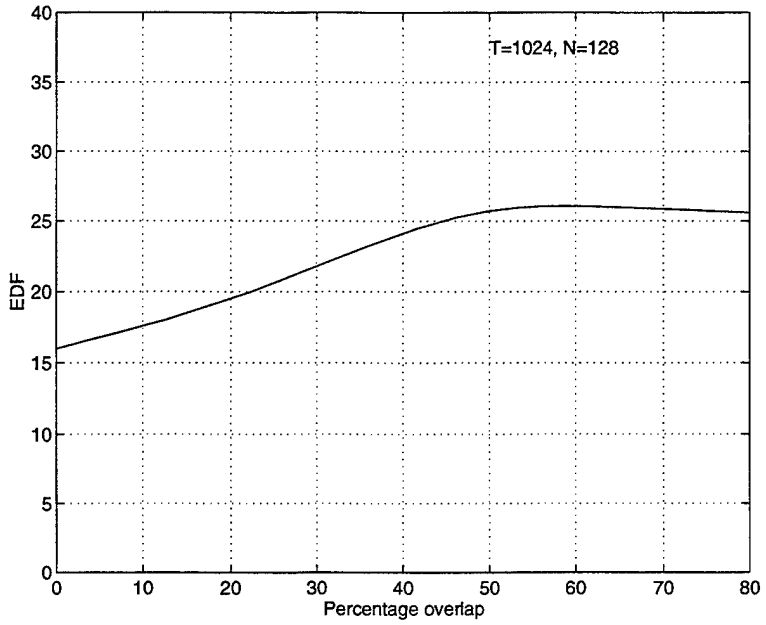

Figure 3. *Kaiser-Bessel Window With Peak Sidelobe Level of -30 dB*

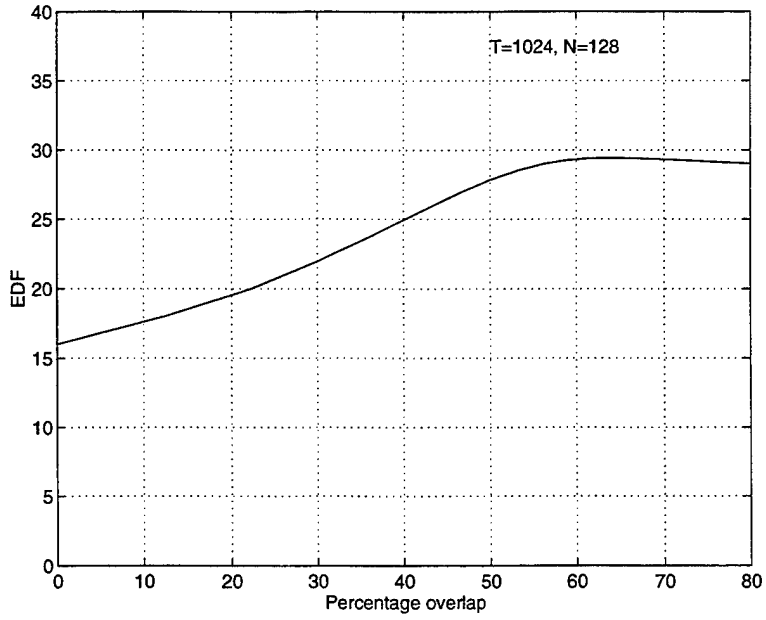

Figure 4. *Kaiser-Bessel Window With Peak Sidelobe Level of -40 dB*

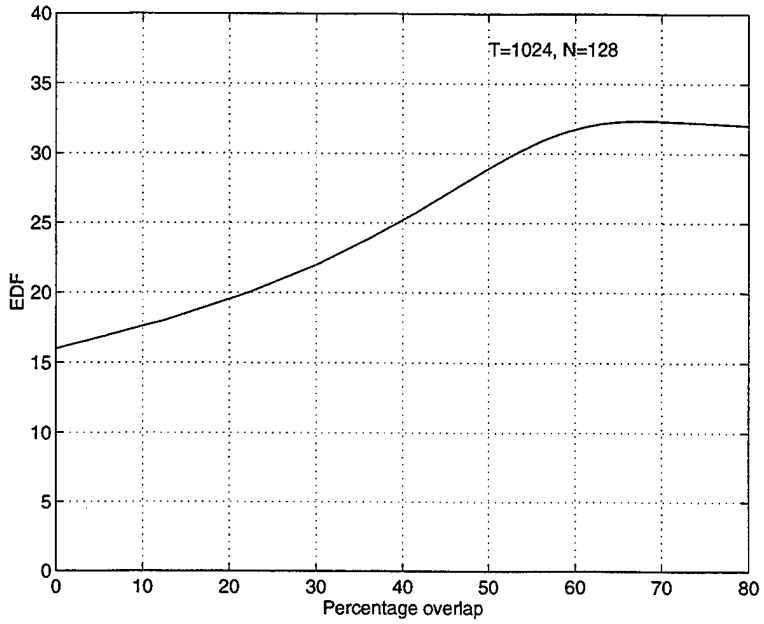

Figure 5. *Kaiser-Bessel Window With Peak Sidelobe Level of -50 dB*

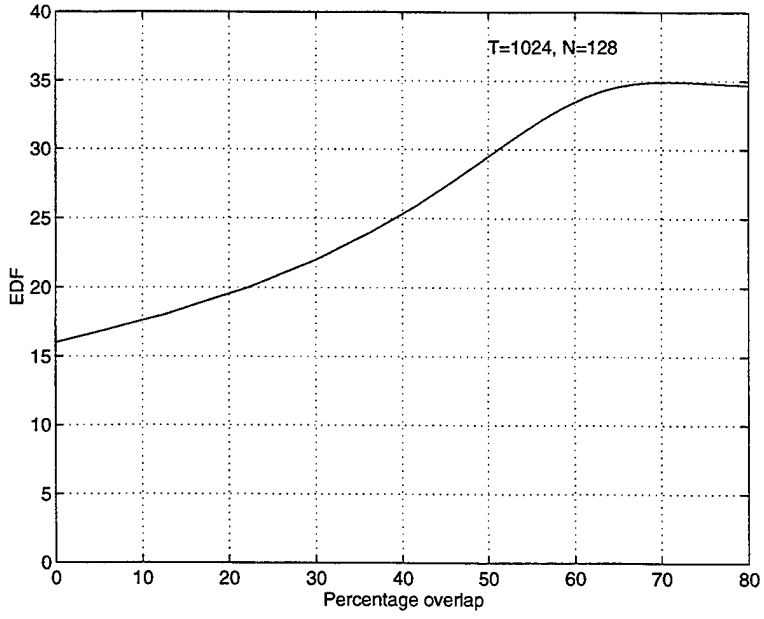

Figure 6. *Kaiser-Bessel Window With Peak Sidelobe Level of -60 dB*

ratio T/N. We find that

$$\max \text{EDF} \approx \left(\frac{T}{N} - \theta\right) \eta \,, \tag{15}$$

where η and θ depend on the type of window and the decibel sidelobe level according to tables 3 and 4. This rather accurate approximation has been verified by examples.

Table 3. *Values of η and θ in the Approximation of Maximum EDF by $\left(\frac{T}{N} - \theta\right) \eta$ for the Kaiser-Bessel Weights*

Sidelobe Level (dB)	Values of η	Values of θ
-40	3.93	0.54
-50	4.35	0.59
-60	4.72	0.63
-70	5.07	0.67

Table 4. *Values of η and θ in the Approximation of Maximum EDF by $\left(\frac{T}{N} - \theta\right) \eta$ for the Dolph-Chebyshev Weights*

Sidelobe Level (dB)	Values of η	Values of θ
-40	3.51	0.49
-50	3.89	0.54
-60	4.25	0.58
-70	4.58	0.61

5. SUMMARY

In this report, we have investigated how to determine the optimal amount of data overlap to produce spectral estimates of maximum stability. For the two types of spectral windows examined, namely, Kaiser-Bessel and Dolph-Chebyshev, the optimal amount of overlap varied from 59 to 93 percent and depended greatly on the ratio T/N, the ratio of the total number of data points available to the number of data points in a segment. In spite of this dependency, it was shown through extensive computation that a 50-percent overlap results in a loss of stability (as measured by the EDF value) of only 1 to 15 percent, with the loss frequently less than 10 percent.

REFERENCES

1. F. J. Harris, "On the Use of Windows for Harmonic Analysis With the Discrete Fourier Transform," *Proceedings of the IEEE*, vol. 66, no. 1, January 1978, pp. 51–83.

2. R. B. Blackman and J. W. Tukey, *The Measurement of Power Spectra*, Dover Publications, Inc., New York, NY, 1959.

3. A. H. Nuttall, "Spectral Estimation by Means of Overlapped FFT Processing of Windowed Data," NUSC Technical Report 4169, Naval Underwater Systems Center, New London, CT, 13 October 1971, p. 22.

APPENDIX A
DERIVATION OF MEAN AND VARIANCE

The power density spectrum estimate is given by equation (10) in conjunction with equation (9). For later use, the crosscorrelation of two different spectral estimates at general analysis frequency f_k is given by the complex ensemble average

$$\begin{aligned} C_{pq} &\equiv \overline{\boldsymbol{y}_p(f_k)\boldsymbol{y}_q^*(f_k)} \\ &= \sum_n \sum_m \overline{\boldsymbol{x}(n\Delta)\boldsymbol{x}^*(m\Delta)}\, w(n-S_p)\, w^*(m-S_q)\, \exp\left[-i2\pi f_k \Delta(n-m)\right] , \end{aligned} \tag{A-1}$$

where we have allowed for complex processes $\boldsymbol{x}(t)$ and complex weights $\{w(n)\}$. When we express correlation $R_x(n\Delta - m\Delta)$ in equation (A-1) in terms of its spectrum $G_x(f)$ according to a Fourier transform, the average becomes

$$\begin{aligned} C_{pq} &= \int df\, G_x(f) \sum_n \exp\left(i2\pi f \Delta n\right)\, w(n-S_p)\, \exp\left(-i2\pi f_k \Delta n\right) \\ &\quad \times \sum_m \exp\left(-i2\pi f \Delta m\right)\, w^*(m-S_q)\, \exp\left(i2\pi f_k \Delta m\right) \\ &= \int df\, G_x(f)\, \left|W(f_k - f)\right|^2 \exp\left[i2\pi (S_q - S_p)\Delta (f_k - f)\right] , \end{aligned} \tag{A-2}$$

where we have used the window definition from equation (6). Note that the only relevant feature of the window is its magnitude-squared value, $|W(f)|^2$, insofar as the crosscorrelation C_{pq} is concerned.

All the functions in equation (A-2) have period $1/\Delta$ in f, except for spectrum $G_x(f)$, which decays with f (and leads to convergence of the integral). Therefore, we can express crosscorrelation C_{pq} in terms of the (double-sided) aliased spectrum

$$G_a(f) \equiv \sum_m G_x\left(f - \frac{m}{\Delta}\right) \quad \text{for all } f \tag{A-3}$$

(which also has period $1/\Delta$ in f) according to

$$C_{pq} = \int_{1/\Delta} df\, G_a(f)\, \left|W(f_k - f)\right|^2 \exp\left[i2\pi (S_q - S_p)\Delta (f_k - f)\right] , \tag{A-4}$$

where we can now integrate over any period of length $1/\Delta$. This is an exact result. Thus, it is always the aliased spectrum $G_a(f)$ that governs the statistics of the spectral estimate $\boldsymbol{Y}(f_k)$ in equation (10). This is a natural consequence of process $\boldsymbol{x}(t)$ being sampled at time increment Δ, and is not due to the particular method of spectral analysis employed.*

If the original stationary random process $\boldsymbol{x}(t)$ is prefiltered by an analogue filter prior to being sampled at time increment Δ seconds, the frequency components in $G_x(f)$ outside the range $-0.5/\Delta$ to $0.5/\Delta$ Hz can be sufficiently suppressed so that the effects of aliasing are negligible. Thus, although there are always replications of $G_x(f)$ in $G_a(f)$ at spacing $1/\Delta$ Hz, through proper prefiltering, their overlap will be insignificant and aliasing effects can be ignored.

A special case of equation (A-4) is given by the autocorrelation value

$$C_{pp} = \int_{1/\Delta} df\, G_a(f)\, |W(f_k - f)|^2 \,, \tag{A-5}$$

which is recognized as the convolution (at analysis frequency f_k) of the aliased spectrum with the magnitude-squared window, the integral being conducted over any period of length $1/\Delta$.

At this point, we assume that the magnitude-squared window $|W(f)|^2$ is narrow enough so that only the value of the aliased spectrum $G_a(f)$ at analysis frequency f_k matters in the integral of equation (A-4). That is, the detail in $G_a(f)$ near f_k is broader than the window width. Then, we obtain the good approximation

$$C_{pq} = G_a(f_k) \int_{1/\Delta} df\, |W(f_k - f)|^2 \exp\left[i2\pi(S_q - S_p)\Delta(f_k - f)\right] . \tag{A-6}$$

The integral in this equation can be simplified by the substitution of the window definition from equation (6) and the interchange of the integral with the two summations, yielding the compact result

$$C_{pq} = \frac{1}{\Delta} G_a(f_k)\, \phi_w\left(S_q - S_p\right) , \tag{A-7}$$

*Sampling $\boldsymbol{x}(t)$ at time increment Δ causes its power spectrum to be periodically reproduced with a period of $1/\Delta$. If Δ is not small enough, these repetitions will overlap, causing aliasing.

where ϕ_w is the autocorrelation of the weight sequence:

$$\phi_w(m) \equiv \sum_n w(n)\, w^*(n-m) \quad \text{for all } m\,. \tag{A-8}$$

In particular, equation (A-7) yields $C_{pp} = \frac{1}{\Delta}\, G_a(f_k)\, \phi_w(0)$ for $1 \le p \le P$.

We can now address the statistics of power spectral estimate $\boldsymbol{Y}(f_k)$ in equation (10). By use of equation (A-1), we have the mean value

$$\text{Av}\{\boldsymbol{Y}(f_k)\} = \frac{1}{P}\sum_{p=1}^{P} C_{pp} = \frac{1}{\Delta}\, G_a(f_k)\, \phi_w(0)\,. \tag{A-9}$$

This result holds regardless of the statistics of process $\boldsymbol{x}(t)$; that is, $\boldsymbol{x}(t)$ need not be Gaussian. Since the absolute scaling is arbitrary, we can select $\phi_w(0) = \Delta$ so that the mean value equals the desired quantity, namely, spectral value $G_a(f_k)$. Then, estimate $\boldsymbol{Y}(f_k)$ would be unbiased.

To evaluate the variance of $\boldsymbol{Y}(f_k)$, we need to assume that the random variables $\{\boldsymbol{y}_p(f_k)\}$ in equation (9) are zero-mean Gaussian; this would happen, for example, if input process $\boldsymbol{x}(t)$ were zero-mean Gaussian. The mean square value of $\boldsymbol{Y}(f_k)$ is then given by

$$\begin{aligned}\overline{\boldsymbol{Y}^2(f_k)} &= \frac{1}{P^2}\sum_{p,q=1}^{P} \overline{\boldsymbol{y}_p \boldsymbol{y}_p^* \boldsymbol{y}_q \boldsymbol{y}_q^*} \\ &= \frac{1}{P^2}\sum_{p,q=1}^{P} \left(\overline{\boldsymbol{y}_p \boldsymbol{y}_p^*}\;\overline{\boldsymbol{y}_q \boldsymbol{y}_q^*} + \overline{\boldsymbol{y}_p \boldsymbol{y}_q}\;\overline{\boldsymbol{y}_p^* \boldsymbol{y}_q^*} + \overline{\boldsymbol{y}_p \boldsymbol{y}_q^*}\;\overline{\boldsymbol{y}_p^* \boldsymbol{y}_q}\right), \end{aligned} \tag{A-10}$$

where we have used the Gaussian character of $\{\boldsymbol{y}_p\}$. The first term in equation (A-10) leads to the square of the mean value in equation (A-9). The second term in equation (A-10) is approximately zero, as may be confirmed by conducting an analysis similar to that of equation (A-2) for $\overline{\boldsymbol{y}_p \boldsymbol{y}_q}$; instead of a magnitude-squared window, we obtain two displaced windows, $W(f_k - f)W(f_k + f)$, which are widely spaced in frequency (except when f_k is equal to a multiple of the Nyquist frequency $\frac{1}{2\Delta}$), thereby resulting in a small output. The third term in equation (A-10) therefore leads to the variance in the form

$$\text{Var}\{\boldsymbol{Y}(f_k)\} = \frac{1}{P^2}\sum_{p,q=1}^{P} |C_{pq}|^2 = \frac{G_a^2(f_k)}{P^2\Delta^2}\sum_{p,q=1}^{P} |\phi_w\,(S_q - S_p)|^2\,, \tag{A-11}$$

where we have used equation (A-7).

The EDF, defined in equation (11), is now available from equations (A-9) and (A-11) as

$$EDF = \frac{2P^2}{\sum_{p,q=1}^{P} \left| \frac{\phi_w(S_q - S_p)}{\phi_w(0)} \right|^2}, \tag{A-12}$$

where the exact values of the aliased spectrum $G_a(f_k)$, the particular analysis frequency f_k, and the sampling increment Δ have canceled out. Thus, the relative stability of the power density spectrum estimate $\boldsymbol{Y}(f_k)$ (of the aliased spectrum) depends only on the shape (not the level) of the weight sequence $\{w(n)\}$ and integer parameter values N, T, and P. The P integer shifts $\{S_p\}$ are given by equations (7) and (8), and depend on the particular number of pieces, P, being considered; see figures 1 and 2 for the method of data processing used here.

APPENDIX B
SOME BANDWIDTH MEASURES FOR DISCRETE WEIGHTING

Various bandwidth measures corresponding to a time-limited weighting function are possible for the window. Here, we will consider three different measures and show how simply they can be computed directly from a set of discrete-time weights without having to compute the frequency domain window itself.

We presume a real and even set of weights $\{w_n\}$, such that $w_{-n} = w_n$; this is different from the weights in the main text, which were one sided and ranged from $w(0)$ to $w(N-1)$. The total number of nonzero weights is N, which is an odd number here. For time sampling increment Δ, the corresponding window is

$$W(f) \equiv \sum_n w_n \exp(-i2\pi f \Delta n) \quad \text{for all } f, \tag{B-1}$$

which has period $1/\Delta$ in frequency f. Also, $W(f)$ is even and real for all f. For future use, we define the Nyquist frequency $F = 1/(2\Delta)$, which is halfway to the first aliasing lobe at $f_s = 1/\Delta$.

The first bandwidth measure is the effective bandwidth f_e, defined as the single-sided (positive frequencies) quantity

$$f_e \equiv \frac{\left(\int_0^F df\, W(f)\right)^2}{\int_0^F df\, W(f)^2} = \frac{\left(\int_{-F}^F df\, W(f)\right)^2}{2\int_{-F}^F df\, W(f)^2}. \tag{B-2}$$

However, these integrals can be expressed in the weighting domain very simply as

$$\int_{-F}^F df\, W(f) = \sum_n w_n \int_{1/\Delta} df\, \exp(-i2\pi f \Delta n) = \frac{1}{\Delta} w_0\,, \tag{B-3}$$

$$\begin{aligned}\int_{-F}^F df\, W(f)^2 &= \sum_{n,m} w_n\, w_m \int_{1/\Delta} df\, \exp[-i2\pi f \Delta (n+m)] \\ &= \frac{1}{\Delta}\sum_n w_n\, w_{-n} = \frac{1}{\Delta}\sum_n w_n^2\,.\end{aligned} \tag{B-4}$$

Substitution in equation (B-2) yields

$$f_e = \frac{1}{2\Delta} \frac{w_0^2}{\sum_n w_n^2} . \tag{B-5}$$

Since there are a total of N weights, taken at time increment Δ, we can define the weighting time duration as $L = N\Delta$, leading to the dimensionless product

$$Lf_e = \frac{N}{2} \frac{w_0^2}{\sum_n w_n^2} . \tag{B-6}$$

Two additional "rectangular" single-sided bandwidth measures that could alternatively be used are given, by means of equations (B-3) and (B-4), as

$$f_1 \equiv \frac{1}{W(0)} \int_0^F df\, W(f) = \frac{1}{2\Delta} \frac{w_0}{\sum_n w_n}, \tag{B-7}$$

$$f_2 \equiv \frac{1}{W(0)^2} \int_0^F df\, W(f)^2 = \frac{1}{2\Delta} \frac{\sum_n w_n^2}{\left(\sum_n w_n\right)^2} . \tag{B-8}$$

Observe that frequency measure f_1 is the geometric mean of the other two measures; that is, $f_1 = \sqrt{f_2 f_e}$, whether obtained from the frequency domain or the time domain relations.

An example of these three bandwidth measures for the Dolph-Chebyshev window, with total number of samples $N = 127$, is shown below in figure B-1, with the actual numerical data supplied in table B-1. The values of Lf_e are computed from equation (B-6); the values for Lf_1 and Lf_2 are computed from the equations obtained by substituting $L = N\Delta$ into equations (B-7) and (B-8), respectively:

$$Lf_1 = \frac{N}{2} \frac{w_0}{\sum_n w_n} , \tag{B-9}$$

$$Lf_2 = \frac{N}{2} \frac{\sum_n w_n^2}{\left(\sum_n w_n\right)^2} . \tag{B-10}$$

We observe in figure B-1 that all three bandwidth measures happen to be equal when the sidelobe level is approximately -23 dB. (Note that all these ordinate numbers in figure B-1 would have been twice as large if we had defined double-sided bandwidth measures in equations (B-2), (B-7), and (B-8).)

There is a reason for the upturn in the Lf_2 curve for the sidelobe levels near -20 dB. For deep sidelobe levels, the squared window $W^2(f)$ generates most of its contribution to the integral in equation (B-8) from the mainlobe region about $f = 0$. However, for shallow sidelobe levels (e.g., -20 dB), where the mainlobe width is rather narrow, a significant contribution to equation (B-8) is also made by the extended sidelobe region. This causes the numerator of equation (B-8) to increase, even though the mainlobe is becoming narrower. An alternative bandwidth measure, such as the half-power bandwidth, would not have this upturn for the shallower sidelobe levels.

Table B-1. *The Three Bandwidth Measures Lf_e, Lf_1, and Lf_2 as a Function of the Sidelobe Level for the 127-Point Dolph-Chebyshev Window*

dB	Lf_e	Lf_1	Lf_2	dB	Lf_e	Lf_1	Lf_2
-20	0.454	0.593	0.774	-52	1.338	0.977	0.714
-22	0.575	0.625	0.678	-54	1.366	0.996	0.726
-24	0.687	0.655	0.624	-56	1.393	1.015	0.739
-26	0.784	0.683	0.596	-58	1.420	1.033	0.751
-28	0.864	0.711	0.584	-60	1.446	1.051	0.764
-30	0.931	0.737	0.583	-62	1.471	1.068	0.776
-32	0.988	0.762	0.588	-64	1.496	1.086	0.788
-34	1.036	0.786	0.597	-66	1.521	1.102	0.799
-36	1.079	0.810	0.608	-68	1.545	1.119	0.811
-38	1.118	0.833	0.620	-70	1.569	1.136	0.822
-40	1.154	0.855	0.634	-72	1.592	1.152	0.833
-42	1.188	0.877	0.647	-74	1.615	1.168	0.844
-44	1.220	0.898	0.660	-76	1.638	1.184	0.855
-46	1.251	0.918	0.674	-78	1.661	1.199	0.866
-48	1.281	0.938	0.687	-80	1.683	1.215	0.877
-50	1.310	0.958	0.701				

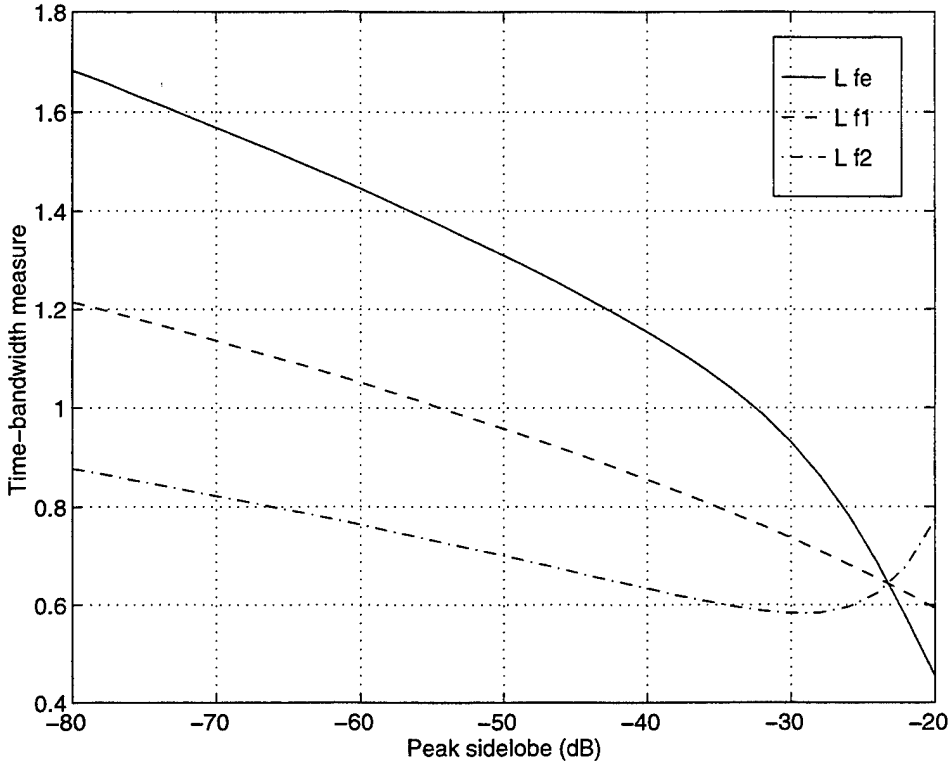

Figure B-1. *Bandwidth Measures for the 127-Point Dolph-Chebyshev Window as a Function of the Sidelobe Level in Decibels*

APPENDIX C
KAISER-BESSEL PROPERTIES FOR CONTINUOUS WEIGHTING

$$\text{Weighting } w(t) = \frac{1}{L} I_0\left(\beta\sqrt{1-4t^2/L^2}\right) \quad \text{for } |t| < \frac{L}{2}\text{; zero otherwise.}$$

$$\text{Window } W(f) = \frac{\sin\left(\sqrt{\pi^2L^2f^2-\beta^2}\right)}{\sqrt{\pi^2L^2f^2-\beta^2}} = \frac{\sinh\left(\sqrt{\beta^2-\pi^2L^2f^2}\right)}{\sqrt{\beta^2-\pi^2L^2f^2}} \quad \text{for all } f.$$

Effective Bandwidth:

$$f_e \equiv \frac{\left[\int_0^\infty df\, W(f)\right]^2}{\int_0^\infty df\, W^2(f)} = \frac{\left[\int df\, W(f)\right]^2}{2\int df\, W^2(f)} = \frac{w^2(0)}{2\int dt\, w^2(t)}\,.$$

$$Lf_e = \frac{I_0^2(\beta)}{2\int_0^{\pi/2} d\theta\, \cos(\theta)\, I_0^2(\beta\cos\theta)}.$$

Half-Power Bandwidth:

$$\frac{W(f)}{W(0)} = \frac{\sinh(x)}{x}\frac{\beta}{\sinh\beta}, \text{ where } x = \sqrt{\beta^2-\pi^2L^2f^2}\,.$$

Define f_h from the equation $\dfrac{W(f_h)}{W(0)} = \dfrac{1}{\sqrt{2}}$.

Solve $\dfrac{\sinh(x_h)}{x_h} = \dfrac{1}{\sqrt{2}}\dfrac{\sinh(\beta)}{\beta}$ for x_h. Then, $Lf_h = \sqrt{\dfrac{\beta^2-x_h^2}{\pi^2}}$.

First Zero Crossing:

$$\pi = \sqrt{\pi^2 L^2 f_z^2 - \beta^2}\,.$$

$$Lf_z = \sqrt{\frac{\beta^2 + \pi^2}{\pi^2}}\,.$$

$$\frac{Lf_z}{2} = \frac{\sqrt{\beta^2 + \pi^2}}{2\pi}\,.$$

The three bandwidth measures Lf_e, Lf_h, and $\frac{1}{2}Lf_z$ are listed as a function of the Kaiser-Bessel parameter β in table C-1. These data are also plotted in figure C-1. Table C-1 and figure C-1 convey the same information for the Kaiser-Bessel weighting as figure B-1 and table B-1 do for the Dolph-Chebyshev weighting.

Table C-1. *The Three Bandwidth Measures Lf_e, Lf_h, and $\frac{1}{2}Lf_z$ as a Function of the Window Parameter β for the Kaiser-Bessel Window*

β	Lf_e	Lf_h	$\frac{1}{2}Lf_z$
2	0.7544	0.4966	0.5927
3	0.9398	0.5467	0.6914
4	1.1006	0.5997	0.8095
5	1.2396	0.6516	0.9398
6	1.3634	0.7011	1.0779
7	1.4763	0.7481	1.2211
8	1.5809	0.7928	1.3679
9	1.6789	0.8352	1.5172
10	1.7713	0.8758	1.6682

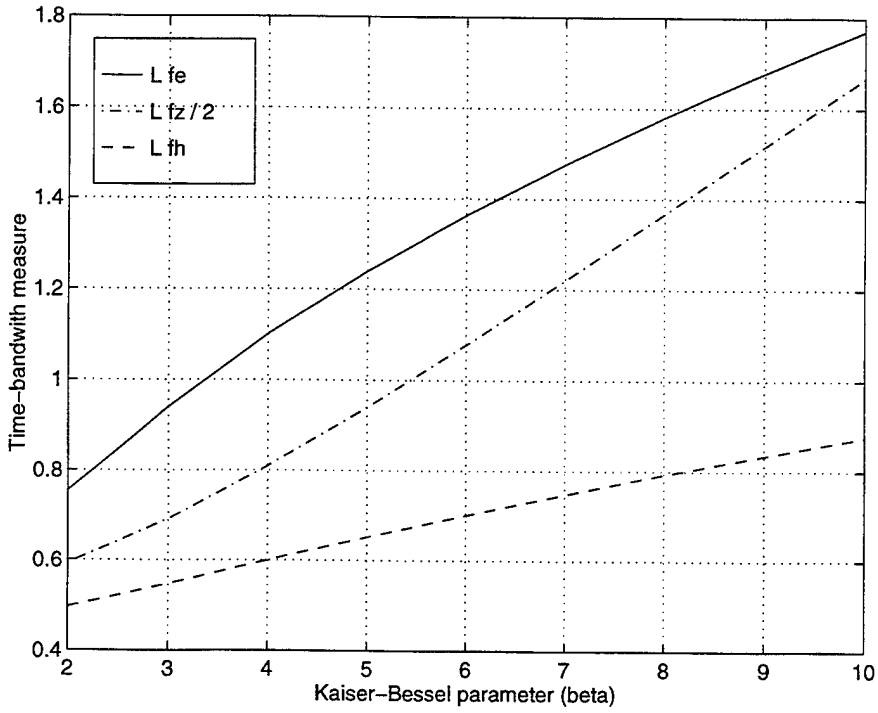

Figure C-1. *Bandwidth Measures for the Kaiser-Bessel Window as a Function of the Window Parameter β*

APPENDIX D
MATLAB CODE TO COMPUTE EDF

This appendix lists the MATLAB code that can be used to compute the EDF for a given windowing function. This code is available from the authors upon request.

```
function [Edf, Fo] = edf(W, N, T, Pm)

% edf.m - evaluates the expected degrees of freedom for a given
%         windowing function for various values of the percentage
%         overlap. The formal parameters are defined as follows.
%
%                 W - temporal weights (N x 1)
%                 N - size of the FFT
%                 T - total number of data points
%                 Pm - maximum number of pieces to be used
%
%         Edf, a Pm x 1 vector, is returned to the calling context,
%         as well as the corresponding values of the fractional overlap
%         in the Px x 1 vector Fo.
%
%                 Edf - expected degrees of freedom (Pm x 1)
%                  Fo - fractional overlap (Pm x 1)
% $Id: compute_edf.tex,v 1.2 1996/09/23 07:23:48 hall Exp hall $

Edf = zeros(Pm, 1);
Fo = zeros(Pm, 1);
S = zeros(Pm, 1);
Phi2 = zeros(N, 1);
N1 = N - 1;
Phi0 = W' * W;                  % dot product of the window W
P2 = Phi0 * Phi0;
Phi2(1) = 1.0;

for Ks = 1:N1
    A = 0.0;
    for Ns = Ks:N1
```

```
        A = A + W(Ns + 1) * W(Ns - Ks + 1);
    end
    Phi2(Ks + 1) = A * A / P2;
end

Edf(1) = 2.0;

% P is the number of pieces of data being used. All of the values
% of EDF for P less than (T/N) are the same because there is no overlap.
for P = (T/N):Pm
    Sc = (T - N) / (P - 1);
    for Ps = 1:P
        S(Ps) = round((Ps - 1) * Sc);
    end
    A = 0.0;
    for Ps = 1:(P-1)
        Sp = S(Ps);
        for Qs=(Ps+1):P
            Ns = S(Qs) - Sp;
            if (Ns < N1)
                A = A + Phi2(Ns + 1);
            end
        end
    end
    Edf(P) = 2 * P * P / (P + 2 * A); % EDF from equation (13)
    Fo(P) = max(0, 1 - Sc / N);       % FO from equation (12)
end
% end of edf.m
```

INITIAL DISTRIBUTION LIST

Addressee	No. of Copies
Naval Sea Systems Command (Thanh Nguyen (PMS 425243))	1
Commander, Submarine Development Squadron 12 (R. Ambrico)	1
Defense Technical Information Center	12
Analysis & Technology, Arlington (H. MacDonald)	1
Analysis & Technology, North Stonington (R. Wise)	1
Analysis & Technology, Engineering Technology Center, Mystic (D. Ghen, E. Dubac)	2